ChemComm

Topological capture of mRNA for silencing gene expression

Journal:	*ChemComm*
Manuscript ID	CC-COM-11-2022-006189.R2
Article Type:	Communication

COMMUNICATION

Topological capture of mRNA for silencing gene expression

Fangjie Lyu,[a] Takashi Tomita, [a] Naoko Abe, [a] Haruka Hiraoka, [a] Fumitaka Hashiya, [a] Yuko Nakashima,[a] Shiryu Kajihara,[a] Fumiaki Tomoike, [b] Zhaoma Shu, [a] Kazumitsu Onizuka,[c] Yasuaki Kimura [*a] and Hiroshi Abe [*a, b, d, e]

Received 00th January 20xx,
Accepted 00th January 20xx

DOI: 10.1039/x0xx00000x

We describe herein topological mRNA capture using branched oligodeoxynucleotides (ODNs) with multiple reactive functional groups. These fragmented ODNs efficiently formed topological complexes on template mRNA in vitro. In cell-based experiments targeting AcGFP mRNA, the bifurcated reactive ODNs showed a much larger gene silencing effect than the corresponding natural antisense ODN.

Antisense technology[1] is useful for target-specific gene knock-down, in which oligonucleotides (ONs) that have a complementary sequence to that of the target mRNA (called antisense ONs) are used as the effector molecules. Antisense ONs hybridize to the target mRNA, and translation from the hybridized mRNA is suppressed due to steric inhibition of ribosomes. Alternatively, RNase H is recruited to the hybridization sites, resulting in the degradation of the target mRNA. Antisense technology is widely used in basic research and for therapeutic applications.[2-5] However, several problems remain[6], such as target specificity, membrane permeability, and low efficacy of gene suppression in some cases. For the last issue, many strategies have been developed, and most of them focus on chemically modified nucleotides that aim to enhance binding to the target mRNA.[7-12] In addition, unique strategies, such as cross-linking antisense ONs [13-18], have been reported. In contrast to these strategies, we envisioned that topological capture of mRNA using reactive ONs would result in a more stable complex than a simple mRNA-antisense duplex. In this regard, we previously developed an automatic pseudorotaxane-forming reaction *in vitro* with fragment DNAs on template DNA or RNA strands, where two types of reactive fragment DNAs were used.[19-21] Each DNA had two reactive functional group (RFG) pairs; one pair had phosphorothioate (PS) and dibenzylcyclooctyne (DBCO), and the other pair had chloroacetamide and azide. The two DNA strands underwent double chemical ligation reactions on the template DNA or RNA to form a pseudorotaxane complex with the template ONs. In light of the robustness of the resulting pseudorotaxane complex, we envisioned that this kind of topological complex formation (TCF) on the target mRNA (Fig. 1B) would result in a higher gene silencing effect than canonical duplex formation by canonical antisense ODNs (Fig. 1A).

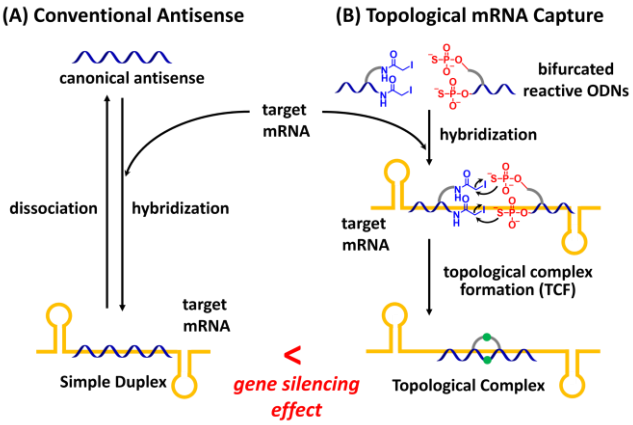

Fig. 1. Conceptual scheme of topological complex formation on the target mRNA resulting in gene silencing. (A) Conventional antisense method. (B) Gene silencing by topological complex formation.

We designed the reactive ON fragments as follows. First, antisense DNA was fragmented at an appropriate position, and the RFGs for chemical ligation were attached at the terminus of each DNA fragment. Additionally, the second or third RFGs were introduced at the terminus of the branches from the backbone DNA to enable multiple chemical ligations for strong topological fixation of the target mRNA. For the RFG pairs, we selected

[a] *Department of Chemistry, Graduate School of Science, Nagoya University, Furo, Chikusa, Nagoya 464-8602, Japan, E-mail: h-abe@chem.nagoya-u.ac.jp.*
[b] *Research Center for Materials Science, Nagoya University, Furo, Chikusa, Nagoya 464-8602, Japan*
[c] *Institute of Multidisciplinary Research for Advanced Materials, Tohoku University 2-1-1 Katahira, Aoba-ku, Sendai, Miyagi 980-8577, Japan.*
[d] *CREST, Japan Science and Technology Agency, 7, Gobancho, Chiyoda-ku, Tokyo 102-0076, Japan*
[e] *Institute for Glyco-core Research (iGCORE), Nagoya University, Furo-cho, Chikusa-ku, Nagoya, Aichi 464-8601, Japan*
† Footnotes relating to the title and/or authors should appear here.
Electronic Supplementary Information (ESI) available: [details of any supplementary information available should be included here]. See DOI: 10.1039/x0xx00000x

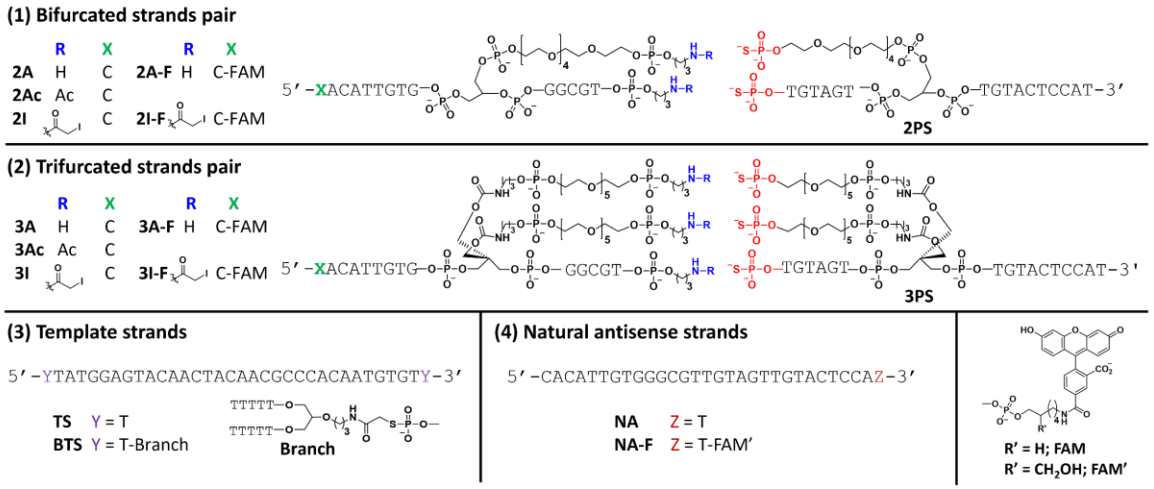

Fig. 2. Structures and sequences of the ONs used in this study.

iodoacetamide (IAc) and PS groups because the templated ligation reaction using these RFGs is rapid.[22-25] As the model target for TCF, we selected the 447-474 site of AcGFP mRNA (747 nt), which was found to be easily accessible by the antisense ODNs in our preliminary studies. The two antisense fragments were designed to be approximately 15 mers so that the melting temperature (Tm) of the duplex was approximately 45 °C (calculated using OligoAnalyzer 3.1 online software from IDT, ONs 0.25 μM, NaCl 50 mM) to ensure efficient hybridization under cell-based conditions. The choice of linker moieties connecting the backbone strand and the additional RFGs is crucial for efficient TCF. On designing the branching position and the linker length between the branching point and the RFGs, we referred to the length of the oligonucleotide duplex pitch and several types of ethylene glycol chains based on molecular modelling (Fig. S4). Based on the calculated 3D structural information, we selected the hexaethylene glycol unit as the linker moiety and positioned the branching position as 5-6 mer internal to the fragmentation terminus. Glycerol or hexaglycerol moieties were selected for the single- or double-branching structure, respectively. The sequences and structures of ODNs used in this study are summarized in Fig. 2. As negative control strands (i.e., non-reactive strands) of IAc-DNAs, the free amino (**2A**, **3A**), and acetyl derivatives (**2Ac**, **3Ac**) were also prepared. These ODNs were purified by reverse-phase HPLC and characterized by MALDI-TOF-MS (Fig. S1).

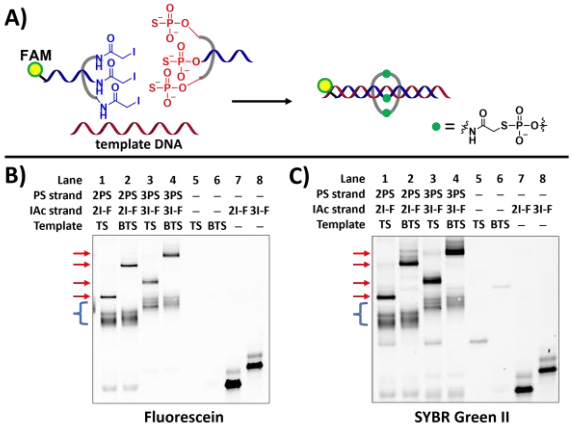

Fig. 3. TCF on DNA template. The reaction was carried out with fluorescence-labeled IAc-DNA (**2I-F** or **3I-F**, 1.0 μM), PS-DNA (**2PS** or **3PS**, 2.0 μM), DNA template (**TS** or **BTS**, 1.5 μM) in phosphate buffer (pH 7.0, 20 mM) containing NaCl (100 mM), DTT (0.2 mM) at 37°C for 1 h. (A) Schematic representation of TCF with **3PS**, **3I-F** and **TS** (B), (C) PAGE analysis of the reactions (10% denaturing PAGE, 6.5 M urea, at 4°C). (B); Detection with fluorescein signal. (C); Stained with SYBR Green II. Bands indicated by red arrows are complexes of the ligated strand and the template DNA. Bands indicated with blue parenthesis are those of ligated strands that have dissociated from the complex.

First, we evaluated whether the designed TCF could proceed using two types of model DNA template (Fig. 3A); one is a 30 mer standard DNA (**TS**) having an identical sequence to that of the target mRNA site, and the other is the same template strand but having additional short branching strands at both termini (**BTS**), which imitates the higher-order structure of mRNA. Fluorescence-labeled IAc-DNAs (**2I-F**, **3I-F**) were used to trace the reaction. The TCF reactions were performed at pH 7.0 and 37ºC for 1 hour, and the resulting mixture was analyzed by denaturing PAGE at 4 °C (Fig. 3B, 3C). Regardless of the presence or absence of branching strands in templates, or the number of branches, the TCF reaction proceeded efficiently to generate the target topological complexes (bands indicated by red arrows). These complexes showed significant band shifts from the starting IAc DNAs (lanes 7,8) and template strands (lanes 5,6). Remarkably, the topological complex was stable enough to be analyzed by denaturing PAGE. The formation of the target complex was confirmed by MALDI-MS analysis of the samples extracted from the bands indicated by the red arrows; the MS peaks of the ligated strand and the template were observed (Fig. S2). The values of only observed MS peaks derived from the reactive ODN pairs matched well with the calculated values, suggesting that the double or triple ligation fully proceeded without any partial ligation reactions in both bifurcated and trifurcated systems, respectively. The dissociation of the template DNA and ligated ODN occurred without breaking the ligated structure based on the observed MS values (Fig. S2). The complexes partially dissociated to give bands of the ligated strand without the template DNA (highlighted with blue parenthesis in Fig. 3B). The yields of the chemical ligation were calculated based on the band intensity of the complex and the dissociated strand, which were 89% (lane 1), 91% (lane 2), and 98% (lanes 3 and 4). A high efficiency of the complex formation

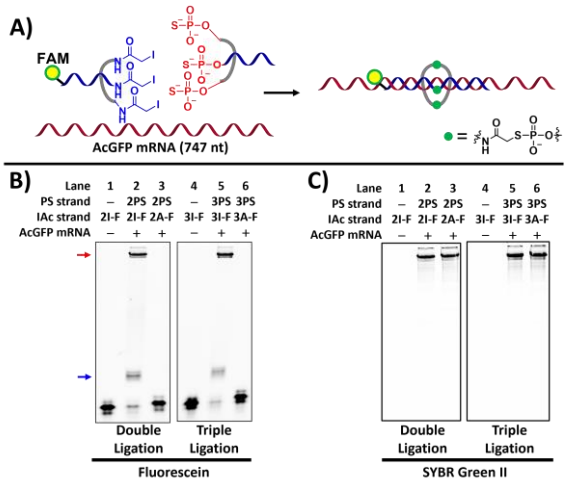

Fig. 4. TCF on AcGFP mRNA. The reaction was carried out with fluorescein-labeled IAc-DNA (**2I-F** or **3I-F**, 1.0 μM), PS-DNA (**2PS** or **3PS**, 3.0 μM), AcGFP1 mRNA (0.45 μg/μL) in phosphate buffer (pH 7.0, 20 mM) containing NaCl (100 mM), DTT (0.2 mM) at 37°C for 1 h. (A) Schematic representation of TCF with **3PS**, **3I-F** and AcGFP mRNA. (B) and (C) PAGE analysis of the reactions (8% denaturing PAGE, 6.5 M urea, at 4ºC) (B) Detection with fluorescein signal. (C) Stained with SYBR Green II. Bands indicated by red arrows are complexes of ligated strand and mRNA. Bands indicated by blue arrows are ligated strands dissociated from the complex.

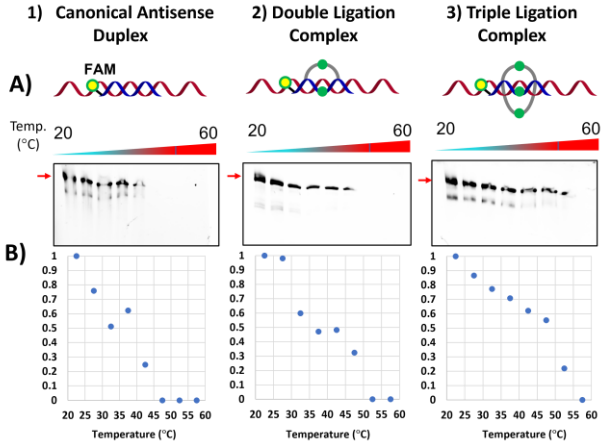

Fig. 5. Evaluation of thermal stability of the complex. The TCF reaction was performed with IAc-DNA (**2I-F** or **3I-F**, 1.5 μM), PS-DNA (**2PS** or **3PS**, 3.0 μM), AcGFP1 mRNA (10 μg/20 μL) in phosphate buffer (pH 7.0, 20 mM) containing NaCl (100 mM) at 37 for 1 h. For the natural antisense strand, **NA-F** (1.5 μM) was used in place of IAc-DNA and PS-DNA. The mixture was analyzed by 5% native PAGE with temperature gradient gel electrophoresis. (A) PAGE results with fluorescence signal detection. Bands indicated with red arrows are those of the topological complexes. (B) Plots of relative band strength of the complex at each temperature.

reaction was also observed for the corresponding 30 nt RNA template strand (Fig. S5).

After confirming the formation of the complex on the model DNA and RNA templates, we next evaluated the TCF reaction on the target AcGFP mRNA (747 nt, Fig. 4A). The TCF reactions were performed at pH 7.0 and 37 °C for 1 hour, and the resulting mixture was analyzed by denaturing PAGE at 4 °C (Figs. 4B, 4C, S8). Again, the TCF reaction proceeded efficiently to yield bands corresponding to the complexes (indicated by a red arrow) along with the dissociated ligated strands (indicated by a blue arrow). The yields of the ligation reactions were 88% for bifurcated ODNs and 91% for the trifurcated ODNs. The peaks corresponding to the ligated strand were confirmed by MALDI-TOF MS analysis of samples isolated from the complex bands (Fig. S3). This dissociation of the pseudorotaxane complex would have proceeded without degradation of mRNA, since no sign of mRNA degradation was observed in both dPAGE analysis and MALDI-TOF MS measurements. According to the previous study on the stability of pseudorotaxane complexes,[19] the complex could reversibly associate and dissociate, even though they could survive dPAGE under specific conditions like those adopted in this study. The MALDI-TOF MS measurements were performed after desalting to observe the uniform peak as proton adduct, and this desalting process would have promoted the dissociation of the complex as observed in the MS measurements. Similarly as in the model DNA case, the complete ligation reaction was confirmed in both the bifurcated and trifurcated reaction systems based on the MS values. (Fig. S3). This highly efficient TCF reaction should be applicable for gene silencing in cells.

Next, the thermal stability of the topological complexes with mRNA was evaluated using temperature gradient gel electrophoresis (TGGE). The fluorescein-labeled IAc strand, PS-strand, and mRNA were mixed at pH 7.0 and incubated for 1 hour.

For the natural antisense, fluorescein-labeled antisense ODNs (**NA-F**) were used in place of IAc and PS ODNs. The mixture was applied to TGGE under native conditions with a temperature gradient ranging from 20 °C to 60 °C (Fig. 5A). The electrophoresis conditions were set so that the complex remained in the gel and the dissociated ligated strands were eluted from the gel. The band intensity at each temperature was normalized to that at 20 °C and the relative band intensity was plotted (Fig. 5B). The temperature range at which the intensity halved was calculated from the graphs; 30 – 35 °C for the natural antisense ODN (**NA-F**), 35 – 40 °C for the bifurcated ODNs (**2I-F** and **2PS**) and 45 –55 °C for the trifurcated ODNs (**3I-F** and **3PS**). These results indicate that the branched reactive ODNs showed higher stability in the duplex than the normal antisense ODN and that the complex stability increased as the number of ligated strands increased.

Finally, the TCF-based gene silencing was evaluated in cells. HeLa cells were transfected with the reactive ODNs and AcGFP vector, and AcGFP expression was evaluated with fluorescence microscopy. As shown in Fig. 6A, the bifurcated ODNs (panel 3) showed a higher level of suppression than the natural antisense ODN (panel 2). It was confirmed that this higher gene silencing effect depended on the ligation reaction because the corresponding non-reactive ODN pair showed almost no suppression (panel 4). For trifurcated ODNs, the suppression level was very low, and the silencing effect was comparable to or less that of natural antisense (panel 2) and non-reactive trifurcated ODNs (panel 6). The gene silencing effects were also evaluated by flow cytometry (Fig. 6B). While the natural antisense showed a 9.5% silencing effect (column 2), the bifurcated ODNs showed a 27% silencing effect (column 3). Again, there was almost no suppression by the non-reactive bifurcated ODNs (column 4), confirming that the superior silencing effect was based on the TCF reaction. Consistent with the microscopy analysis, the trifurcated ODNs showed a much weaker silencing effect (5.8%, column 5) than the bifurcated

ODNs. We conducted an *in vitro* RNase H assay to determine whether the silencing effect was mediated by the RNase pathway, which was performed after forming the pseudorotaxane complex on AcGFP mRNA (Fig. S6A). Interestingly, we observed RNase H-mediated mRNA degradation for the bifurcated and trifurcated TCF system, although partially, with a different cleavage pattern than that of natural antisense ODN. This result would reflect the sterical effect of the pseudorotaxane on RNase H. There was little difference in cleavage efficiency between the bifurcated and trifurcated system (Fig. S6B). These results indicate that natural antisense ODN is more RNase H-dependent than the bifurcated pseudorotaxane system in knockdown activity. We attribute the strong knockdown activity of the bifurcated pseudorotaxane system partially to the steric effect. Given that once the pseudorotaxane complex was formed on the target mRNA, the trifurcated complex was more thermodynamically stable (Fig. 5), had nearly the same efficiency in RNase H-mediated cleavage as the bifurcated complex (Fig. S6), and the ligation reaction on the template mRNA is very efficient (Fig. 4), this unexpected result might be because the trifurcated ODNs were less efficient in accessing the target mRNA in a complex intracellular environment, presumably due to higher sterical hindrance. The silencing effect by the bifurcated ODNs was not inferior to that by a 2'-MOE-based gapmer antisense ODN fully modified with phosphorothioate (Fig. S7).

In conclusion, we have developed a TCF reaction on target mRNA with bifurcated or trifurcated reactive ODNs. TCF on target ONs was confirmed by PAGE and MALDI-TOF-MS analysis. The reaction was sufficiently efficient to yield the target complex almost quantitatively within 1 hour *in vitro*. The thermal stability of the topological complexes was evaluated by temperature gradient gel electrophoresis, and the triple-ligation complex showed the highest stability. The bifurcated reactive ODNs targeting of AcGFP in cells showed a much higher gene silencing effect than that of the corresponding natural antisense, demonstrating the validity of the TCF strategy for greater gene silencing effects. A study examining a more elaborated TCF design for higher gene silencing effects is underway.

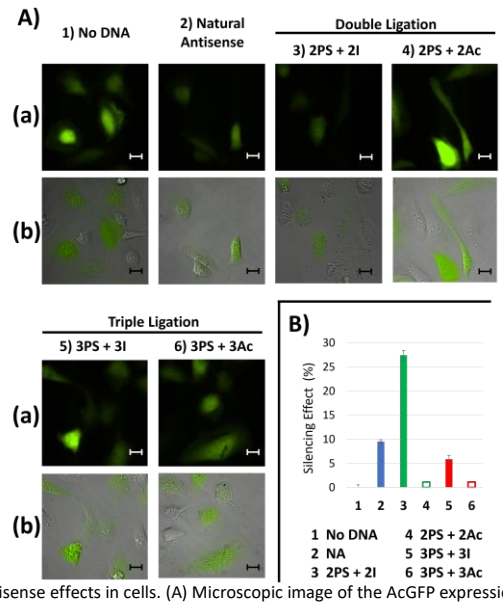

Fig. 6. Antisense effects in cells. (A) Microscopic image of the AcGFP expression in HeLa cells. (a) Fluorescence images (b) Merge of DIC and fluorescence images. Scale bar 20 μm. Hela cells were administrated with AcGFP1 C1 pDNA (0.25 μg/μL) and antisense strands. **NA** (entry 2, 1 μM) or the combination of PS-DNA (**2PS** or **3PS**) and amino-DNA (**2I**, **2Ac**, **3I**, **3Ac**) (entries 3-6, 1 μM each) were used. (B) Suppression rate of AcGFP in HeLa cells based on flowcytometry analysis. AcGFP1 C1 pDNA (0.125 μg/μL), pLL×mcherry pDNA (0.125 μg/μL) were administrated with **NA** (1 μM) or the combination of PS-and amino-DNA (1 μM). Data represent the mean ± s.d. for 3 replicates.

Conflicts of interest

There are no conflicts to declare.

Notes and references

1. B. M. Paterson, B. E. Roberts, and E. L. Kuff, *Proc. Natl. Acad. Sci.* 1977, **74**, 4370-4374.
2. K. F. Pirollo, A. Rait, L. S. Sleer and E. H. Chang, *Pharmacology & Therapeutics*, 2003, **99**, 55-77.
3. R. Malik and I. Roy, *Expert Opin. Drug Discov.*, 2008, **3**, 1189-1207.
4. M. Y. Skoblov, *Molecular Biology*, 2009, **43**, 917-929.
5. V. K. Sharma, R. K. Sharma and S. K. Singh, *MedChemComm*, 2014, **5**, 1454-1471.
6. R. Juliano, J. Bauman, H. Kang and X. Ming, *Molecular Pharmaceutics*, 2009, **6**, 686-695.
7. N. M. Bell and J. Micklefield, *ChemBioChem*, 2009, **10**, 2691-2703.
8. T. P. Prakash, *Chemistry & Biodiversity*, 2011, **8**, 1616-1641.
9. G. F. Deleavey and M. J. Damha, *Chem. & Biol.*, 2012, **19**, 937-54.
10. M. L. Jain, P. Y. Bruice, I. E. Szabo and T. C. Bruice, *Chemical Reviews*, 2012, **112**, 1284-1309.
11. V. K. Sharma, P. Rungta and A. K. Prasad, *RSC Advances*, 2014, **4**, 16618-16631.
12. A. Khvorova and J. K. Watts, *Nat. Biotech.*, 2017, **35**, 238.
13. H. Maruenda and M. Tomasz, *Bioconjug. Chem.*, 1996, **7**, 541-4.
14. S. Imoto, T. Hori, S. Hagihara, Y. Taniguchi, S. Sasaki and F. Nagatsugi, *Bioorg. Med. Chem Lett.*, 2010, **20**, 6121-6124.
15. F. Nagatsugi and S. Imoto, *Organic & Biomolecular Chemistry*, 2011, **9**, 2579-2585.
16. S. Hagihara, S. Kusano, W.-C. Lin, X.-G. Chao, T. Hori, S. Imoto and F. Nagatsugi, *Bioorg. Med. Chem Lett.*, 2012, **22**, 3870-3872.
17. S. Kusano, T. Haruyama, S. Ishiyama, S. Hagihara and F. Nagatsugi, *Chem. Commun.*, 2014, **50**, 3951-3954.
18. L. L. G. Carrette, E. Gyssels, N. De laet and A. Madder, *Chemical Communications*, 2016, **52**, 1539-1554.
19. K. Onizuka, F. Nagatsugi, Y. Ito and H. Abe, *Journal of the American Chemical Society*, 2014, **136**, 7201-7204.
20. K. Onizuka, T. Chikuni, T. Amemiya, T. Miyashita, K. Onizuka, H. Abe and F. Nagatsugi, *Nucleic Acids Res.*, 2017, **45**, 5036-5047.
21. K. Onizuka, T. Miyashita, T. Chikuni, M. Ozawa, H. Abe and F. Nagatsugi, *Nucleic Acids Res.*, 2018, **46**, 8710-8719.
22. S. M. Gryaznov and R. L. Letsinger, *Journal of the American Chemical Society*, 1993, **115**, 3808-3809.
23. M. K. Herrlein and R. L. Letsinger, *Nucleic Acids Res.*, 1994, **22**, 5076-5078.
24. H. Abe, Y. Kondo, H. Jinmei, N. Abe, K. Furukawa, A. Uchiyama, S. Tsuneda, K. Aikawa, I. Matsumoto and Y. Ito, *Bioconjugate Chemistry*, 2008, **19**, 327-333.
25. H. Maruyama, Y. Nakashima, S. Shuto, A. Matsuda, Y. Ito and H. Abe, *Chem. Commun.*, 2014, **50**, 1284-1287.